Journal Pre-proofs

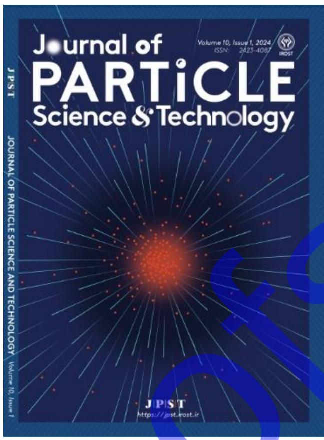

Analytical evaluation of high power ultrasonic assisted cold compaction of titanium powder

Vahid Fartashvand, Amir Abdullah, Rezvan Abedini, Nader Parvin

DOI: https://doi.org/10.22104/jpst.2026.8304.1292
Manuscript number: JPST-2605-1292

To appear in: *Journal of Particle Science and Technology (JPST)*

Received Date: 29 May 2026
Received Date in revised form: 21 July 2026
Accepted Date: 23 July 2026

Please cite this article as: Fartashvand, V., Abdullah, A., Abedini, R., Parvin, N., Analytical evaluation of high power ultrasonic assisted cold compaction of titanium powder, *Journal of Particle Science and Technology* (2025), doi: https://doi.org/10.22104/jpst.2026.8304.1292

Analytical Evaluation of High Power Ultrasonic Assisted Cold Compaction of Titanium Powder

Vahid Fartashvand[1,*], Amir Abdullah[2], Rezvan Abedini [3], Nader Parvin[4]

[1] Department of Industrial Design, Faculty of Art, Alzahra University, Tehran, Iran
[2] Department of Mechanical Engineering, Amirkabir University of Technology, Tehran, Iran
[3] Department of Mechanical Engineering, University of Science and Technology, Tehran, Iran
[4] Materials and Metallurgical Engineering Department, Amirkabir University of Technology, Tehran, Iran

Abstract

Researchers have considered powder compaction modeling to predict necessary compaction pressure at desirable density. This paper presented cold compaction modeling of titanium powder under high-power longitudinal ultrasonic vibration based on experimental tests. Superimposing high-frequency, high-power mechanical vibration on the compaction process could improve green density and density distribution. For this purpose, a special ultrasonic assisted cold compaction setup was designed and fabricated. CP titanium powder with size of < 45 µm compacted (up to 900 MPa) at different ultrasonic powers (0, 100 W, 150 W, 200 W, 300 W). Then, a mathematical formulation was presented for ultrasonic-assisted cold powder compaction consisting of four terms: initial density, particle rearrangement, particle deformation, and ultrasonic vibration effects. The results showed that the presented mathematical model could predict accurately green compact density as a function of compaction pressure and ultrasonic power.

Keywords: CP Titanium, Cold compaction, Ultrasonic vibration, Compaction model

1. Introduction

Titanium and its alloys have been widely used in many industries owing to their unique density, high corrosion resistance, biocompatibility and relative strength [1]. Due to the high cost of these materials, powder metallurgy is a routine method for producing their components [2]. Die pressing at room temperature and then vacuum sintering is a cost-efficient technology of powder technology. During cold compaction, the metal powder is forced (such as titanium) into a desired shape in the die at room temperature by applying high mechanical pressure, without employing any external heat. This process relies on mechanical force to rearrange and deform particles so they stick together. After filling the die by powders (initial density), the pressure pushes the loose particles into the empty spaces between them. This is a particle arrangement phase. As pressure increases, the particles themselves begin to change shape. Metallic particles deform plasticly, flattening out and spreading against each other, creating a large contact area. In brittle materials, particles may undergo fragmentation to fill the voids. The irregular shapes of the particles become locked together [3]. However, die wall friction restricts obtaining high density [4]. Also, density distribution was not uniform along the thickness of compact [5]. These defects cause severe distortion, dimensional instability, and non-uniform mechanical properties after the sintering process. In addition, die wall friction increases the ejection force of compact and consequently increases the wear of tools and shortens their life [5-6,7]. Imposing high power ultrasonic vibration during the cold compaction process causes friction reduction at contacting surfaces [8] as well as acoustic softening [9] of material which leads to better compressibility of powders [10]. Therefore, near full-density sintering parts could be produced due to high green density. Selecting suitable compaction pressure and ultrasonic power is critical to achieving desirable compact density. High compaction load shortens tool life and needs to high tonnage press which increases the cost of the process. This paper aims to find an analytical relationship between the density of titanium compact as a function of compaction pressure and ultrasonic vibration powers.

Researchers have developed and used powder compaction models to calculate the required compaction pressure to achieve a specific density in the conventional cold compaction process. An accurate model should be considered all densification mechanisms. A comprehensive list of mathematical compaction models was reported in [11].

Gerdemann and Jablonski [12] proposed the new compaction equation for conventional cold compaction of titanium powders (Eq. (1)). This model includes three terms for the description of initial density (D_0), particle rearrangement ($A(1-e^{-ap})$) and work-hardening ($B(1-e^{-bp})$) mechanisms contribution on densification of powders.

$$D = D_0 + A(1-e^{-ap}) + B(1-e^{-bp}) \quad [1]$$

The coefficients A and B are the maximum contribution of powder rearrangement and powder deformation on densification, respectively. The a and b constants represent the rate of the powder particle rearrangement and plastic deformation mechanisms. Maximum relative density according to this model is the sum of A, B and D_0. Machaka and Chikwanda [13] evaluated this model for compaction of titanium powders. They explained the physical interpretation of model constants. They reported good agreement with this model by experimental data.

Chen *et al.* [14] used the Panelli-Filho formulation (Eq. (2)) to predict the relative density versus compaction pressure of Ti-6Al-4V titanium alloy. They found good agreement between experimental and mathematical data. In this equation, coefficient A indicates the powder's ability to densification due to plastic deformation.

$$\ln\left(\frac{1}{1-D}\right) = A\sqrt{P} + \ln\left(\frac{1}{1-D_0}\right) \quad [2]$$

Lou *et al.* [15] used the modified Cooper–Eaton equation to simulate the densification behavior of CP titanium powder. They reported that the contribution of particle rearrangement is in the range of 0-200 MPa of compaction pressure and plastic deformation occurred in the range of 200-900 MPa. Machaka and Chikwanda [11] investigated Jones, Heckel, modified Heckel, Panelli-Filho, Ge, Shapiro-Kopopicky, Kawakita-Ludde, Adams-McKeown, Zwan-Siskens, Cooper-Eaton, Gerdemann-Jablonski equations for cold compaction of CP titanium and sponge Titanium powders. The modified Heckel, Ge, and Shapiro-Kopopicky compaction models demonstrate good applicability over all ranges of compaction pressure.

Cheng *et al.* [16], evaluated the Heckel, Huang Peiyun, Cooper and Eaton, and Gerdemann and Jablonski equations by fitting them to experimental data of titanium hydride powder and hydrogenated-dehydrogenated titanium powder compaction. According to their work, All the equations could fit the experimental data well. Tang *et al.* [17] used the Gerdemann–Jablonski and Cooper–Eaton equation to simulate the powder compaction of Unsaturated Titanium Hydride Powders. Aoyagi *et al.* [18] studied modified the Gibson-Ashby formula to predict the compressive strength of porous Ti6Al4V alloys. The work helps establish a prediction equation for materials designed for biomedical applications. Xun *et al.* [19] used Kawakita, Shapiro, and Heckel compression equations to evaluate the compaction behavior of mixed titanium-nickel powders.

Up to date, no analytical modeling for ultrasonic assisted cold compaction of titanium powders has been published. So, this research presents a mathematical model for CP titanium powder's ultrasonic-assisted cold compaction behavior. This model presents an analytical relationship among ultrasonic power, compaction pressure and green density. It decreases the cost of experimental tests for finding suitable compaction and ultrasonic power parameters.

2. Experimental procedure

Commercially pure titanium (CP-Ti) powders were used for this work. The morphology of the titanium powder is shown in Fig. 1 which illustrates the CP-Ti particles are irregular and angular shapes. Picture was captured using a Philips XL30 Scanning Electron Microscope (SEM). Particle size of powders was measured by the laser diffractometry (Model 2000; Mastersizer, Malvern). The result was illustrated in Fig 2. Philips X Unique II XRF device was used to measure the chemical composition of the powders and results are provided in the Table 1. AISI 1.2379 cold work steel die with Ø12.7 mm hole was used for the compaction experiments at room temperature. A universal testing machine (DTU-900MHA) was used to compact powders. Compaction load was recorded by load cell and punch displacement was measured by extensometer. For each compaction experiment, 2.5 g powder was weighed out by digital scale (resolution: 0.001 g) and poured into the die hole. Therefore, the aspect ratio (H/D) of compacts was approximately 0.5.

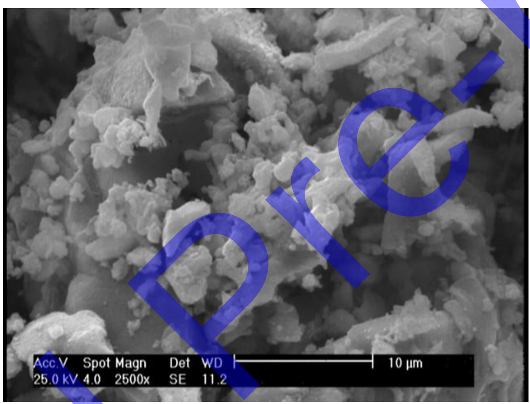

Fig. 1. Morphology of the CP-Ti powder (X2500).

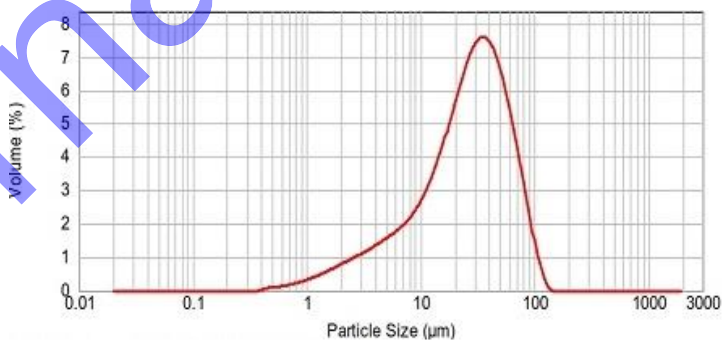

Fig. 2. Particle size distribution of the CP-Ti powder.

Table 1. Chemical composition of CP-Ti powder (wt %).

Element	Ti	S	Fe
Amount (%)	99.26	0.01	0.73

3. Results and discussion

The densification curves of CP powders for different ultrasonic powers are shown in Fig. 3. As shown from Fig. 4, the relative density increases with increasing pressure. The relative density increases rapidly at the initial stages and then the densification rate decreases for all compaction conditions. This phenomenon is due to strain and geometric hardening that makes further deformation difficult. Also, as seen from the curves, there is a considerable difference between initial relative densities for different ultrasonic power. At 20 MPa compaction pressure, relative density is 0.425, 0.508, 0.519, 0.535 and 0.565 for 0 W, 100 W, 150 W, 200 W and 300 W average ultrasonic powers, respectively. It is calculated that relative density increases by about 19.53 %, 22.12 %, 25.88 % and 32.94 % under 20 MPa at 100 W, 150 W, 200 W and 300 W average ultrasonic powers, respectively. This improvement is due to the influence of ultrasonic vibration on the slip and rearrangement of the powders and higher density was achieved at low compaction pressure. This is the advantage of superimposed high power ultrasonic vibration. The relative density at 900 MPa is 0.765, 0.773, 0.774, 0.778 and 0.774 at 0 W, 100 W, 150 W, 200 W and 300 W average ultrasonic powers. It seems that the green density of ultrasonic assisted compacted parts under high compaction pressure (900 MPa) approximately are identical and higher than conventional cold compaction so that 100 W ultrasonic vibration improves the final density of specimens by about 1.05 %.

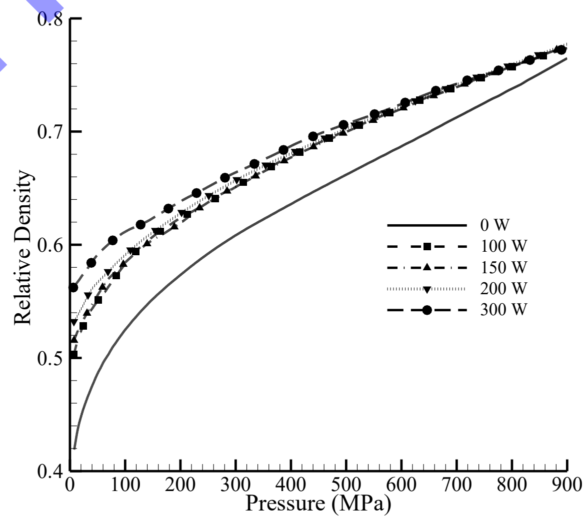

Fig. 3. Compaction curves of CP titanium under different ultrasonic powers.

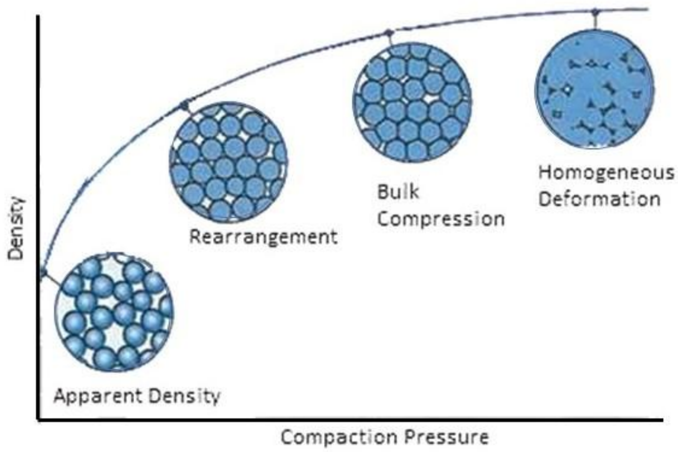

Fig. 4. Effect of compaction pressure on relative density [20].

Recently, Gerdemann–Jablonski [12] presented a new equation that accurately predicts titanium powder compaction, including three terms for considering initial density, particle rearrangement, and plastic deformation. They reported that particle rearrangement contributed to densification until about 100MPa and plastic deformation is the prominent mechanism for further densification. By using this formulation, the contribution of each mechanism in densification of titanium powders is shown in Fig. 5 for conventional compaction. We assumed that D_0 was the initial density at the beginning of data recording (7.9 MPa compaction pressure). In Ref. [12] the authors calculated this parameter from curve fitting, but regarding physical meaning of this parameter, it was considered the initial density at the beginning of data acquisition. Term $A(1 - e^{-ap})$ is related to particle rearrangement and its contribution is high at the initial stages of densification and then its effect reaches a constant amount after approximately 200 MPa. It is reported [21] that for a particle pack with an initial density of 0.64, particle rearrangement contribution in densification is about 40 %. Particle rearrangement contribution diminished over a high-pressure range and plastic deformation is the dominant mechanism in this pressure range. Also, particle fragmentation is not considered because it isn't the main mechanism in titanium (ductile) powder densification [22].

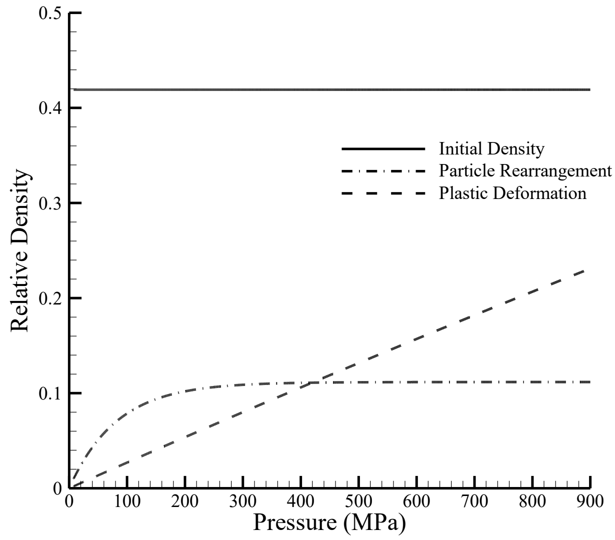

Fig. 5. Contribution of densification mechanism on relative density of CP titanium at conventional cold compaction.

Ultrasonic vibration could improve all of these mechanisms. High power ultrasonic vibration reduces the friction at contacting surfaces which prevent from further densification. Reduction of friction forces improves particle rearrangement. This reduction was attributed to the reduction of coefficient of friction, the reduction of inter-particle contact time, the particles resonance and normal force reduction. Also, ultrasonic vibration reduces flow stress that helps to further plastic deformation. This phenomenon was attributed to acoustic stress superposition theory and energy absorption in material discontinuities such as dislocations. Nevill and Brotzen [23] reported that the decrease in plastic yield limit is independent of the frequency (in the range of 15–80 kHz) and temperature (in the range of 30–500 °C) and preliminary deformation. Some literatures stated that amount of flow stress reduction is proportional to ultrasonic amplitude [23,24,25], while some others reported that this amount is related to ultrasonic intensity [26,27,28,29]. It should be noted that acoustic intensity is proportional to the square of the amplitude. Also, it is assumed that acoustic softening occurs as soon as ultrasonic imposing and ends by stoppage of ultrasonic vibration although some researchers reported residual acoustic softening.

By regarding that ultrasonic effect decreases by increasing of compaction pressure, an exponential term is added to Eq. (1) in order to includes ultrasonic vibration effect.

$$D = D_0 + A(1 - e^{-ap}) + B(1 - e^{-bp}) + C(W)e^{-c(W)P} \quad [3]$$

Which coefficients of D_0, A, a, B and b are assumed the same as Eq. (1) for ultrasonic assisted compaction process. Then, by subtracting the densification curves of conventional compaction from ultrasonic assisted compaction, the contribution of ultrasonic vibration could be clarified for all tests and values of C and c can be determined by curve fitting for each test. Fig. 6 shows that higher ultrasonic power helps to obtain higher ultrasonic contribution until 600 MPa and then their effect is similar.

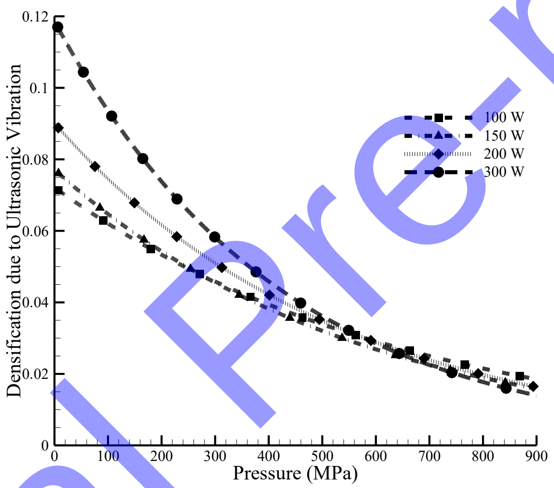

Fig. 6. Contribution of ultrasonic vibration on relative density of CP titanium under ultrasonic assisted cold compaction.

By fitting of $C(W)e^{-c(W)P}$ equation from all curves of Fig. 6, the coefficients of C and c can be found versus ultrasonic power. Then, by fitting suitable curve from these values (Fig. 7 and Fig. 8), Eq. (4) and Eq. (5) describe behavior of these coefficients versus ultrasonic power.

$$C = e^{0.459 \times Log(W) - 4.796} \quad [4]$$

$$R^2 = 0.9891$$

$$c = e^{0.402 \times Log(W) - 8.359} \quad [5]$$

$$R^2 = 0.9972$$

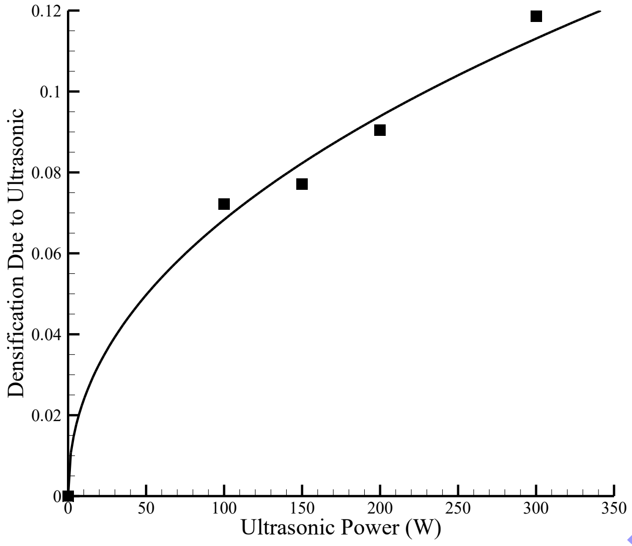

Fig. 7. Variation of coefficient C versus ultrasonic power.

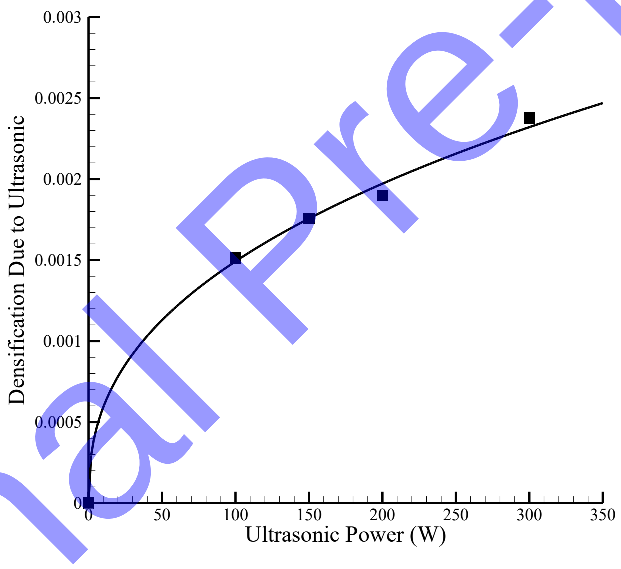

Fig. 8. Variation of coefficient *c* versus ultrasonic power.

Results of mathematical model and experimental data are shown in Fig. 9 to Fig. 12. As shown from these figures, the proposed model shows a good agreement with experimental data over the compaction pressure range. The compaction pressure range 0-900 MPa and ultrasonic power 0-300 W are limitation range of this model for titanium powders.

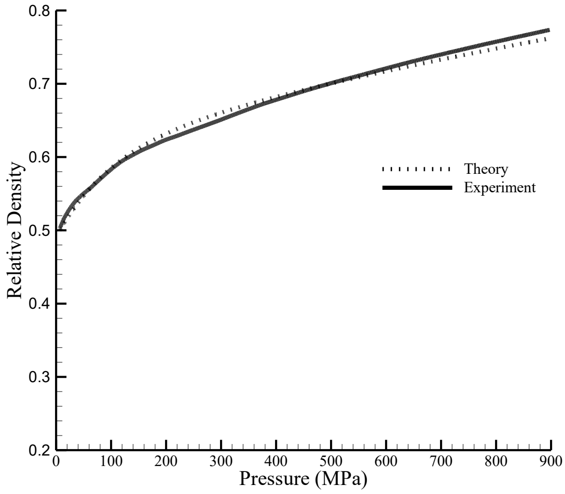

Fig. 9. Comparison of mathematical and experimental data for cold compaction under 100 W ultrasonic power.

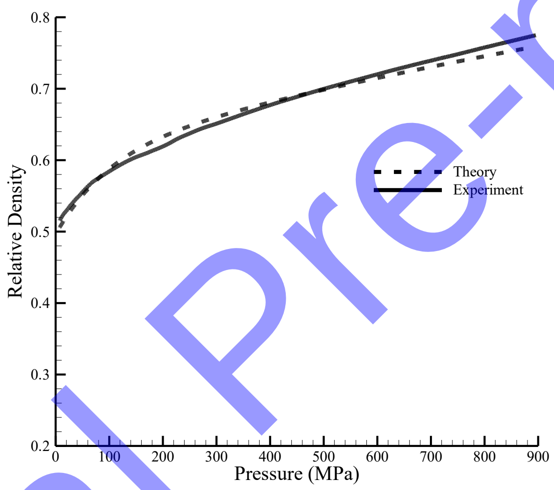

Fig. 10. Comparison of mathematical and experimental data for cold compaction under 150 W ultrasonic power.

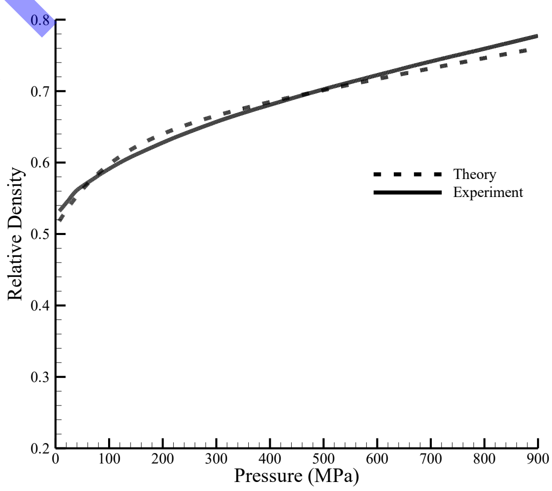

Fig. 11. Comparison of mathematical and experimental data for cold compaction under 200 W ultrasonic power.

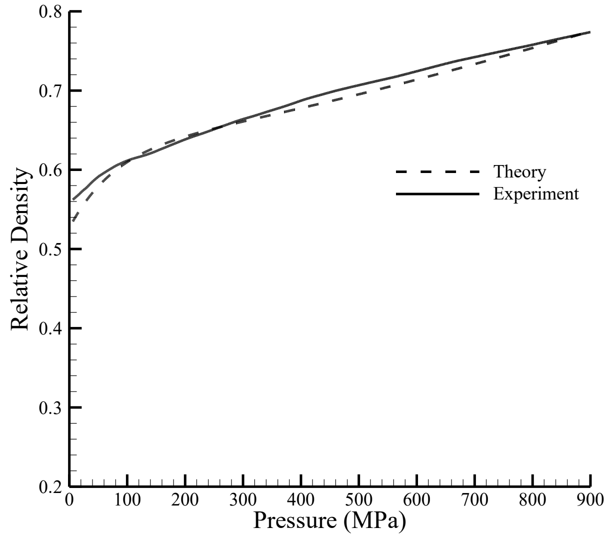

Fig. 12. Comparison of mathematical and experimental data for cold compaction under 300 W ultrasonic power.

By extrapolating the developed theoretical model up to high pressure about 2000 MPa (Fig. 13), it is concluded that at this range of compaction load the densification due to ultrasonic vibration is very small which is shown that longitudinal ultrasonic vibrations damp under high static pressure. With regard to this superposition theory about ultrasonic vibration influence mechanism, it can be concluded that dynamic component of acoustic stress versus static stress is very small and can't affect significantly compaction process. So, the main advantage of superimposing ultrasonic vibration on cold compaction is obtaining higher density at lower compaction pressure.

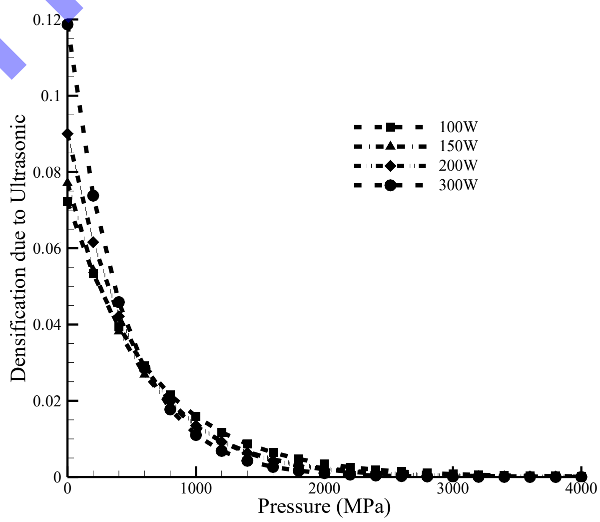

Fig. 13. Variation of ultrasonic effect on densification versus pressure.

4. Conclusion

An analytical model for ultrasonic assisted cold compaction of CP titanium powder based on Gerdemann and Jablonski model was presented that is the sum of four mechanism: initial density, particle rearrangement, particle deformation and ultrasonic vibration effect. We proposed exponential term for ultrasonic effect on green density so that increasing compaction caused to decrease of ultrasonic effectiveness. Ultrasonic vibrations improve particle rearrangement and cause to acoustic softening in bulk deformation steps. The developed model accurately predicts green density as function of compaction pressure and ultrasonic power. This model optimizes the compaction pressure to obtain maximum green density without wasting energy.

Acknowledgments

The authors would like to thank Dr. Yunes Alizadeh, Professor of Amirkabir University of Technology, for his helpful advice on conducting the experiments.

References

[1] Donachie, M. J. (2000). *Titanium: A Technical Guide* (2nd ed.). ASM International, pp. 1-7. https://doi.org/10.31399/asm.tb.ttg2.t61120001

[2] Froes, F. H., Mashl, S. J., Hebeisen, J. C., Moxson, V. S., & Duz, V. A. (2004). The Technologies of Titanium Powder Metallurgy. *The Journal of The Minerals, Metals & Materials Society*, 56, 46-48. https://doi.org/10.1007/s11837-004-0252-x

[3] Qian, M. (2010). Cold compaction and sintering of titanium and its alloys for near-net-shape or preform fabrication. *International Journal of Powder Metallurgy*, 46, 29-44.

[4] Zahraee, S. M. (2016). Experimental Investigation of Metal Powder Compaction without Using Lubricant. *Journal of Particle Science and Technology*, 2(3), 141-149. https://doi.org/10.22104/jpst.2016.445

[5] Hong, S. T., Hovanski, Y., Lavender, C. A., & Weil, K. S. (2008). Investigation of Die Stress Profiles. During Powder Compaction Using Instrumented Die. *Journal of Materials Engineering and Performance, 17*, 382-386. https://doi.org/10.1007/s11665-008-9229-1

[6] Lou, J., Gabbitas, B., & Zhang, D. L. (2013). The Effects of Lubrication on the Density Gradient of Titanium Powder Compacts. *Key Engineering Materials, 551*, 86-91. https://doi.org/10.4028/www.scientific.net/KEM.551.86

[7] Esteban, P. G., Thomas, Y., Baril, E., Ruiz-Navas, E. M., & Gordo, E. (2011). Study of Compaction and Ejection of Hydrided-Dehydrided Titanium Powder. *Metals and Materials International, 17*, 45-55. https://doi.org/10.1007/s12540-011-0207-z

[8] Fartashvand, V., Abedini, R., Khanmohammadi, R., Abdullah, A., & Parvin, N. (2024). Ultrasonic Assisted Cold Compaction of CP Titanium and Ti-6Al-4V Alloy. *Journal of Particle Science and Technology*, *10*(2), 87-96. https://doi.org/10.22104/jpst.2024.7089.1262

[9] Fartashvand, V., Abdullah, A., & Vanini, S. A. S. (2017). Investigation of Ti-6Al-4V Alloy Acoustic Softening. *Ultrasonics Sonochemistry, 38*, 744-749. https://doi.org/10.1016/j.ultsonch.2016.07.007

[10] Khasanov, O. L., & Dvilis, E. S. (2008). Net shaping nanopowders with powerful ultrasonic action and methods of density distribution control. *Advances in Applied Ceramics*, *107*(3), 135-141. https://doi.org/10.1179/174367508X297830

[11] Machaka, R., & Chikwanda, H. K. (2015). Analysis of the Cold Compaction Behavior of Titanium Powders: A Comprehensive Inter-Model Comparison Study of Compaction Equations. *Metallurgical and Materials Transactions A, 46*, 4286-4297. https://doi.org/10.1007/s11661-015-3038-6

[12] Gerdemann, S. J., & Jablonski, P. D. (2011). Compaction of Titanium Powders. *Metallurgical and Materials Transactions A, 42*, 1325-1333. https://doi.org/10.1007/s11661-010-0520-z

[13] Machaka, R., & Chikwanda, H. K. (2015). An Experimental Evaluation of the Gerdemann-

Jablonski Compaction Equation. *Metallurgical and Materials Transactions A, 46*, 2194-2200. https://doi.org/10.1007/s11661-015-2793-8

[14] Chen, W., Yamamoto, Y., Peter, W. H., Gorti, S. B., Sabau, A. S., Clark, M. B., Nunn, S. D., Kiggans, J. O., Blue, C. A., Williams, J. C., Fuller, B., & Akhtar, K. (2011). Cold Compaction Study of Armstrong Process Ti–6Al–4V Powders. *Powder Technology, 214*(2), 194-199. https://doi.org/10.1016/j.powtec.2011.08.007

[15] Lou, J., Gabbitas, B., Zhang, D., & Yang, F. (2015). Effects of Initial Powder Compact Thickness, Lubrication, and Particle Morphology on the Cold Compaction Behavior of Ti Powder. *Metallurgical and Materials Transactions A*, 46, 3646-3655. https://doi.org/10.1007/s11661-015-2925-1

[16] Dong, Sh., Qiu, F., Lei, P., Cheng, T., Ma, G., Qu, L., & Ivasishin, O. 2022). Evaluation and Parameter Analysis of Compaction Equations Applied to Titanium Powder., *Powder Metallurgy, 65*(3), 181-199. https://doi.org/10.1080/00325899.2021.1973654

[17] Luo, L., Sun, Y., & Tang, Y. (2023). Cold Compaction Behavior of Unsaturated Titanium Hydride Powders: Validation of Two Compaction Equations. *Metals*, *13*(2), 360. https://doi.org/10.3390/met13020360

[18] Kimura, K., Aoyagi, N., Sorimachi, T., Miyata, M., & Galindo, T. (2025). Evaluation of Compressive Strength for Sintered Porous Titanium Alloy and Composites with Biopolymers. *Journal of the Japan Society of Powder and Powder Metallurgy, 72*, S923-S929. https://doi.org/10.2497/jjspm.15P-T13-03

[19] Xun, L., Zhong, H., Xinzhi, W., & Xiaobo, H. (2026). A Useful Method to Characterize the Compaction Properties of Ti_2Ni and $TiNi_3$ Mixed Powders. *Shape Memory and Superelasticity, 12*, 300-309. https://doi.org/10.1007/s40830-026-00610-y

[20] Kalpakjian, S., & Schmid, S. R. (2006). *Manufacturing Engineering and Technology* (5th ed.). Prentice Hall.

[21] Liu, J., & Delo, D. P. (2001). Particle Rearrangement During Powder Compaction. *Metallurgical and Materials Transactions A, 32*, 3117-3124. https://doi.org/10.1007/s11661-001-0186-7

[22] Panelli, R. & Filho, F. A. (2001). A Study of a New Phenomenological Compacting Equation, *Powder Technology, 114*(1-3), 255-261. https://doi.org/10.1016/S0032-5910(00)00207-2

[23] Nevill, J. F. & Brotzen, F. R. (1957). The Effect of Vibrations on the Static Yield Strength of Low-Carbon Steel. *Proceedings-American Society for Testing and Materials, 57*, 751-758.

[24] Yao, Z., Kim, G. Y., Wang, Z., Faidley, L., Zou, Q., Mei, D., & Chen, Z. (2012). Acoustic Softening and Residual Hardening in Aluminum: Modeling and Experiments. *International Journal of Plasticity, 39*, 75-87. https://doi.org/10.1016/j.ijplas.2012.06.003

[25] Huang, H., Pequegnat, A., Chang, B. H., Mayer, M., Du, D., & Zhou, Y. (2009). Influence of Superimposed Ultrasound on Deformability of Cu. *Journal of Applied Physics, 106*, 113514. https://doi.org/10.1063/1.3266170

[26] Langenecker, B. (1966). Effects of ultrasounds on deformation characteristics of metals, *IEEE Transactions on Sonics and Ultrasonics, 13*, 1-8. https://doi.org/10.1109/t-su.1966.29367

[27] Green, R. E. (1975). Non-Linear Effects of High-Power Ultrasonics in Crystalline Solids. *Ultrasonics, 13*, 117-127. https://doi.org/10.1016/0041-624X(75)90063-3

[28] Siddiq, A., & El Sayed, T. (2012). A Thermomechanical Crystal Plasticity Constitutive Model for Ultrasonic Consolidation. *Computational Materials Science, 51*, 241-251. https://doi.org/10.1016/j.commatsci.2011.07.023

[29] Wen, T., Wei, L., Chen, X., & Pei, C. L. (2011). Effects of Ultrasonic Vibration on Plastic Deformation of AZ31 During the Tensile Process. *International Journal of Minerals, Metallurgy, and Materials*, *18,* 70-76. https://doi.org/10.1007/s12613-011-0402-4